DINCON 2019 ID: 1938
XIV CONFERÊNCIA BRASILEIRA DE DINÂMICA, CONTROLE E APLICAÇÕES
25 de novembro a 27 de novembro de 2019 – São Carlos/SP

Robust Recursive Regulator and H_∞ Controllers Applied on a Dual-Arm Free-Floating Space Manipulator

José Nuno Almeida Dias Bueno[1]
Rayza Araújo Bezerra[2]
Valdir Grassi Jr[3]
Marco Henrique Terra[4]

Department of Electrical and Computer Engineering

Sao Carlos School of Engineering, USP, Sao Carlos, SP

Abstract. This paper focuses on aspects of the Robust Recursive Linear Quadratic Regulator when applied on a dual-arm planar free-floating space manipulator. The complexities originated from the dynamic coupling between floating base and arms were avoided by using the Dynamic Equivalent Manipulator method in the modelling step. Since reference trajectories were defined in workspace, the Generalized Jacobian was applied to map trajectory points into joint space. For the sake of comparison, we confront our results with a robust H_∞ controller via computational simulations and, based on performance indexes, we conclude that the Robust Recursive Linear Quadratic Regulator had better performance accomplishing trajectory tracking control.

Keywords. Robotic systems. Space manipulators. Robust control. Robust recursive regulator. Dynamically equivalent manipulator.

1 Introduction

Space manipulators have attracted more attention in space operations due to their capability of assisting or even replacing astronauts during tasks such as maintenance, capture and transportation of objects. More specifically, free-floating space manipulators (FFSM) arouse great interest for their characteristics and challenges they bring up for control engineers. During space operations the attitude and translation control systems of the base are turned off, so that the manipulator and the base become dynamically coupled. In other words, the base moves freely in reaction to movements of the robot arm and vice versa. Thus, the problem of trajectory tracking gains higher complexity once it is

[1]bueno.nuno@usp.br
[2]rayza.araujo@usp.br
[3]vgrassi@sc.usp.br
[4]terra@sc.usp.br

necessary to consider such dynamic coupling. Different control systems were already studied for space manipulators applications. Adaptive, robust and other classes of controllers were applied successfully in free-floating prototypes to perform control tasks in joint and workspace [2], [5]. This paper considers the Robust Recursive Linear Quadratic Regulator, proposed in [7], to accomplish tracking control of trajectories defined in workspace for a dual-arm free-floating space manipulator. The modelling was made with the Dynamically Equivalent Manipulator (DEM) method [3], in order to avoid inverse kinematics problems, the concept of Generalized Jacobian Matrix [8] was used to map points from workspace into joint space. This work is organized as follows: section 2 explains the modelling process with the DEM; section 3 defines the control problem for the manipulator; section 4 introduces the Robust Recursive Linear Quadratic Regulator; in section 5 the Generalized Jacobian and its application on the FFSM are presented and explained; section 6 shows simulation parameters and obtained results; finally, in section 7 conclusions are made about the applied methods and about their performances.

2 Dynamically Equivalent Manipulator

The idea of the DEM consists in modelling a free-floating manipulator with n joints through a fixed-base underactuated manipulator with $n+1$ joints. The first joint of the equivalent model is spheric and passive and it is fixed on the center of gravity (CG) of the real robot, while the end-effector (EF) of the DEM is always connected to the EF of the FFSM. Modelling the FFSM through the DEM results in the following kinematic properties [3]: **1)** the axis u_i and $u_i^{'}$ of the i-th joints of DEM and FFSM, respectively, are parallel; **2)** the variables $q_i^{'}$ and q_i describing the motion of the i-th joints of DEM and FFSM, respectively, are equal; **3)** the EFs of DEM and FFSM have the same motion during operation. Furthermore, the relation among geometric parameters of both manipulators necessary to ensure kinematic equivalence between them is given by $W_1' = R_1$, $W_i' = R_i + L_i$, $l_{c1}' = 0$, $l_{ci}' = \frac{\sum_{k=1}^{i-1} m_k}{M_t} L_i$, $i = 2, ..., N$, where W_i' and l_{ci}' are the length of the i'-th link and the distance from the axis of joint J_i' to the CG of the i'-th link of the DEM, respectively; L_i is the distance from the axis of joint J_i to the CG of the i-th link of the FFSM, R_i is the distance from the CG of the i-th link to the axis of joint J_{i+1} of the FFSM, and m_k and M_t are the mass of the k-th link and the total mass of the FFSM, in that order. The necessary conditions to guarantee dynamic equivalence between DEM and FFSM are the relations among masses and inertia moments of both manipulators given by $m_i' = \frac{M_t^2 m_i}{\sum_{k=1}^{i-1} m_k \sum_{k=1}^{i} m_k}$, $I_i' = I_i$, $i = 2, ..., N$. These equivalences result in equivalent kinematic and rotational energies for both DEM and FFSM.

This paper considers the planar FFSM depicted in Fig. 1, with the following structural parameters in the form of $\begin{bmatrix} m_i & I_i & |R_i| & |L_i| \end{bmatrix}$ in SI units: **link 1)** $[1.01, 0.01, 0.112, 0.112]$; **link 2)** $\begin{bmatrix} 1.38 & 0.02 & 0.111 & 0.144 \end{bmatrix}$; **link 3)** $\begin{bmatrix} 4.78 & 0.04 & 0.150 & 0.150 \end{bmatrix}$; **link 4)** $[1.38, 0.02, 0.111, 0.144]$; **link 5)** $[1.01\ 0.01\ 0.112\ 0.112]$. A DEM maps the motion of only one EF of the real robot, thus two DEMs are necessary to model the FFSM, as shown in Fig. 1.

In Table 1 we lay out the equivalences between joint variables of the FFSM and the

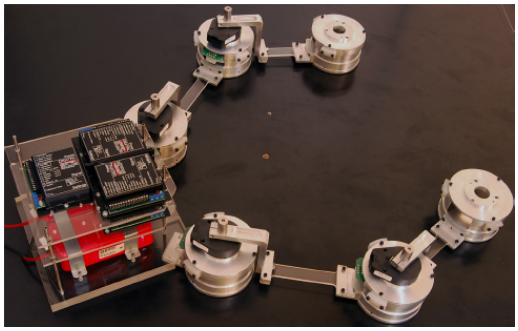

(a) Source: [4].

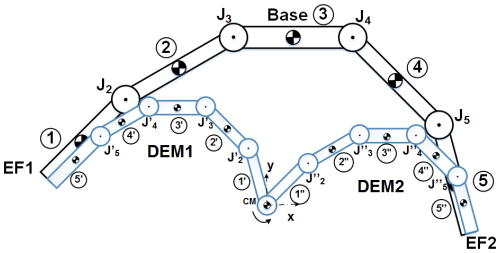

(b) Source: [1].

Figure 1: Planar dual-arm FFSM and the corresponding representation with the DEMs that will map both of its end-effectors.

two DEMs, which preserves the symmetry of the developed model and allows us to control one of the DEMs in such way that the torques to be applied on joints of the second DEM are obtained as a consequence [1].

Table 1: Equivalence between angles and joints of FFSM and DEMs

FFSM	DEM1	DEM2	FFSM	DEM1	DEM2
θ_2	$-\theta'_5$	θ''_2	J_2	J'_5	J''_2
θ_3	$-\theta'_4$	θ''_3	J_3	J'_4	J''_3
θ_4	$-\theta'_3$	θ''_4	J_4	J'_3	J''_4
θ_5	$-\theta'_2$	θ''_5	J_5	J'_2	J''_5

3 Problem Formulation

Since the DEMs have each one passive joint, these will be considered free joints and only the active ones will be controlled. For simplicity, frictional and gravitational forces are neglected and the dynamic equation of a DEM is written as $M(q)\ddot{q}+V(q,\dot{q})+\tau_{dist}=\tau$, where τ are torques applied on joints, τ_{dist} are the disturbance torques, $M(q)$ is the inertia matrix, $V(q,\dot{q})$ is the non-inertial torques and Coriolis matrix. Now, the states of the system are the trajectory tracking errors $x=\begin{bmatrix}e & \dot{e}\end{bmatrix}^T$, and additionaly $\dot{x}=\begin{bmatrix}\dot{e} & \ddot{e}\end{bmatrix}^T$, where $e=\begin{bmatrix}q_d-q & \dot{q}_d-\dot{q}\end{bmatrix}^T$. Solving the dynamic equation for $\ddot{q}$ and replacing it in the second line of $\dot{x}$ results in $\ddot{e}=\ddot{q}_d+M^{-1}(V+\tau_{dist}-\tau)$. Thence, control and disturbance inputs, denoted by u and w respectively, can be defined as $u=\ddot{q}_d+M^{-1}(V-\tau)$ and $w=M^{-1}\tau_{dist}$. The control signal u is determined by the chosen control law, and isoalting τ it is possible to obtain the computed torques to be applied on the joints for trajectory tracking. Thus, the state-space model is given by $\dot{x}=\begin{bmatrix}\dot{e}\\ \ddot{e}\end{bmatrix}=\begin{bmatrix}0 & I\\ 0 & 0\end{bmatrix}\begin{bmatrix}e\\ \dot{e}\end{bmatrix}+\begin{bmatrix}0\\ I\end{bmatrix}u+\begin{bmatrix}0\\ I\end{bmatrix}w$. In practical operations, the system is subject to disturbances and uncertainties, and these factors might significantly degrade the performance of the controller. Hence, robust strategies such as the RLQR and H_∞ are needed to solve the trajectory tracking problem.

4 Robust Recursive Linear Quadratic Regulator

Authors in [7] proposed a Robust Recursive Linear Quadratic Regulator (RLQR) for the discrete-time system subject to parametric uncertainties $x_{i+1} = (F_i + \delta F_i)x_i + (G_i + \delta G_i)u_i$, $x_0 = constant$, where $i = 0, \ldots, N$, $x_i \in \Re^n$ is the state vector, $u \in \Re^m$ is the control input, $F_i \in \Re^{n\times n}$ and $G_i \in \Re^{n\times m}$ are known model matrices, δF_i and δG_i represent parametric uncertainties. The uncertainty matrices are defined as $\begin{bmatrix}\delta F_i & \delta G_i\end{bmatrix} = H_i \Delta_i \begin{bmatrix}E_{F_i} & E_{G_i}\end{bmatrix}$, where $i = 0, \ldots, N$, $H_i \in \Re^{n\times p}$, $E_{F_i} \in \Re^{l\times n}$ and $E_{G_i} \in \Re^{l\times m}$ are known matrices and $\Delta_i \in \Re^{p\times l}$ is an arbitrary matrix such that $||\Delta|| \leq 1$. In order to obtain the robust recursive regulator, it is necessary to solve the following optimization problem [7]:

$$\underset{x_{i+1},u_i}{min} \; \underset{\delta F_i,\delta G_i}{max} \begin{bmatrix}x_{i+1}\\ u_i\end{bmatrix}^T \begin{bmatrix}P^r_{i+1} & 0\\ 0 & R_i\end{bmatrix} \begin{bmatrix}x_{i+1}\\ u_i\end{bmatrix} + \Phi^T \begin{bmatrix}Q_i & 0\\ 0 & \mu I\end{bmatrix} \Phi \tag{1}$$

with fixed $\mu > 0$, $Q_i, R_i \succ 0$ and $\Phi = \left\{ \begin{bmatrix}0 & 0\\ I & -G_i - \delta G_i\end{bmatrix} \begin{bmatrix}x_{i+1}\\ u_i\end{bmatrix} - \begin{bmatrix}-I\\ F_i + \delta F_i\end{bmatrix} x_i \right\}$. For $\mu > 0$, the solution to the optimization problem in Eq. (1) is $\begin{bmatrix}x^*_{i+1} & u^*_i\end{bmatrix}^T = \begin{bmatrix}L_i & K_i\end{bmatrix}^T x_i$, where $i = 0, \ldots, N$ and L_i and K_i are obtained from the recursion

$$\begin{bmatrix}L_i\\ K_i\end{bmatrix} = \begin{bmatrix}0 & 0\\ 0 & 0\\ 0 & 0\\ 0 & 0\\ I & 0\\ 0 & I\end{bmatrix}^T \begin{bmatrix} P^{-1}_{i+1} & 0 & 0 & 0 & I & 0\\ 0 & R_i^{-1} & 0 & 0 & 0 & I\\ 0 & 0 & Q_i^{-1} & 0 & 0 & 0\\ 0 & 0 & 0 & \Sigma_i\left(\mu, \hat{\lambda}_i\right) & \mathcal{I} & -\mathcal{G}_i\\ I & 0 & 0 & \mathcal{I}^T & 0 & 0\\ 0 & I & 0 & -\mathcal{G}^T & 0 & 0 \end{bmatrix}^{-1} \begin{bmatrix}0\\ 0\\ -I\\ \mathcal{F}_i\\ 0\\ 0\end{bmatrix}, \tag{2}$$

where $\Sigma_i = \begin{bmatrix}\mu^{-1} I - \hat{\lambda}_i^{-1} H_i H_i^T & 0\\ 0 & \hat{\lambda}_i^{-1} I\end{bmatrix}$, $\mathcal{I} = \begin{bmatrix}I\\ 0\end{bmatrix}$, $\mathcal{G}_i = \begin{bmatrix}G_i\\ E_{G_i}\end{bmatrix}$, and $\mathcal{F}_i = \begin{bmatrix}F_i\\ E_{F_i}\end{bmatrix}$.

5 Generalized Jacobian

Proposed by [8], the Generalized Jacobian relates EF velocities to active joints velocities in a way that the calculation of such variables does not depend on passive joint variables. For an underactuated manipulator with $n = n_a + n_p$ joints, with n_a active and n_p passive, the dynamic equation can be rewritten as

$$\begin{bmatrix}M_p & M_{pa}\\ M^T_{pa} & M_a\end{bmatrix} \begin{bmatrix}\ddot{q}_p\\ \ddot{q}_a\end{bmatrix} + \begin{bmatrix}V_p\\ V_a\end{bmatrix} = \begin{bmatrix}0\\ \tau_a\end{bmatrix} + \begin{bmatrix}J^T_p\\ J^T_a\end{bmatrix} F_{ext}, \tag{3}$$

where q_a e q_p are the angles of active and passive joints, respectively, M_p, M_{pa}, M^T_{pa} and M_a are inertia matrices, V_p and V_a are non-inertial and Coriolis matrices, τ_a is the torque vector of the active joints, J^T_a and J^T_p are jacobian matrices related to active and passive joints, respectively, and F_{ext} are disturbance forces actuating on the EF.

Velocities of the EF are given in function of joint velocities as $\dot{\chi} = J_a \dot{q}_a + J_p \dot{q}_p$. It is possible to eliminate variables of passive joints by integrating the first line in Eq. (3) and

replacing it in $\dot{\chi}$, resulting in $\dot{\chi} = \hat{J}\dot{q}_a + J_p D_p^{-1}(D_p\dot{q}_p + D_{pa}\dot{q}_a)$. A condition of zero initial momentum was imposed, so $J_p D_p^{-1}(D_p\dot{q}_p + D_{pa}\dot{q}_a) = 0$. For the FFSM and the DEMs used in the modelling step, the velocities of EFs are related to the velocities of active joints of the DEMs by $\dot{\chi}_{EFi} = \hat{J}_{DEMi}\,\dot{q}_{a_{MDEi}}$, where $\hat{J}_{DEMi}$ is the Generalized Jacobian matrix of the i-th DEM. The symmetries that resulted from the modelling step made possible to gather both generalized jacobian matrices in a single equation, so the velocities of EFs of the FFSM and active joints of DEM2 are related as demonstrated in [1]. The reader should refer to [1] in order to have a better understanding on this topic. Lastly, trajectories were defined in the workspace of the FFSM and mapped into the joint space of the DEMs by such relation. Thus, we do not need to deal with the inverse kinematics problem.

6 Simulation and results

Simulations were made in Matlab with a sampling time of $10^{-4}s$. The disturbance applied on the joints are represented by torques of the form $\tau_{d_i}(t) = Ae^{\frac{(t-t_{med})^2}{2\sigma^2}} sen(2\pi ft)$ as in [6], where $A = [0.001\ 0.08\ 0.08\ 0.1\ 0.1]N.m$ are the maximum amplitude of the disturbance in each joint, $t_{med} = 2.5s$, $\sigma = 2.5$ and $f = 2Hz$. Results are exhibited just for DEM2 to avoid redundant figures, since the the results for DEM1 are obtained through the symmetries from Table 1. The reference trajectory for EF1 is a straight line defined by $x_d(t) = a_0 + a_1t + a_2t^2 + a_3t^3 + a_4t^4 + a_5t^5$, and $y_d(t) = y_0 + (x_d(t) - x_0)(y_f - y_0)(x_f - x_0)^{-1}$. Given the boundary conditions at initial ($t = t_0$) and final ($t = t_f$) times, the coefficients for this fifth order polynomial can be easily obtained. For EF2 a quintuple curve was defined by $x_d(t) = a_0 + a_1t + a_2t^2 + a_3t^3 + a_4t^4 + a_5t^5$ and $y_d(t) = b_0 + b_1x_d + b_2x_d^2 + b_3x_d^3 + b_4x_d^4 + b_5x_d^5$. Analogously to the straight line trajectory, from initial and final conditions the coefficients a_k and b_k, $k = 0, 1, ..., 5$, are obtained. The boundary conditions are, respectively, $(x_{0_{EF1}}, y_{0_{EF1}}, x_{0_{EF2}}, y_{0_{EF2}}) = (-0.61, -0.11, 0.61, 0, 14)m$ and $(x_{f_{EF1}}, y_{f_{EF1}}, x_{f_{EF2}}, y_{f_{EF2}}) = (-0.40, 0, 0.40, 0, 30)m$; $(\dot{x}_d(t_0), \dot{y}_d(t_0)) = (\dot{x}_d(t_f), \dot{y}_d(t_f)) = (0, 0)$; $(\ddot{x}_d(t_0), \ddot{y}_d(t_0)) = (\ddot{x}_d(t_f), \ddot{y}_d(t_f)) = (0, 0)$. Also, $t_0 = 0$ and $t_f = 5s$, and within this period disturbance torques τ_{d_i} were applied on the joints. The resulting reference trajectories and desired motion of the FFSM are shown in Fig. 2.

RLQR: parameters and weighting matrices selected for the numerical simulation with the RLQR were $H_i = \begin{bmatrix} h_1 & h_2 & \dots & h_n \end{bmatrix}^T$, with $h_i \in [-0.3, 0.3]$, $i = 1, ..., n$, $\Delta = 1.0$, $\mu = 10^{15}$, $Q = diag(80000, 70000, 70000, 11000, 11000, 11000, 100, 100, 3000, 2000)$, and $R = diag(0.01, 0.005, 0.05, 0.0001, 0.0001, 0.01, 0.005, 0.05, 0.0001, 0.0001)$, so the elements of the state-space matrices were changed up to 30% from nominal values to represent parametric uncertainties. Elements of E_F and E_G are equal to the elements of the main diagonal of F_i and G_i, respectively.

Robust H_∞: the considered robust H_∞ controller was proposed by authors in [6] and the following parameters were adopted for the computational simulation: $K_p = 300$, $K_d = 100$, $M_s = 10$, $\omega_b = 10^{-5}rad/s$, $E = 0.0001$, $M_u = 150$ and $\omega_{bc} = 10^6 rad/s$. To represent parametric uncertainties, masses and moments of inertia of the manipulator were changed also up to 30% from nominal values. The reader should refer to [6] in order to understand how such parameters were inserted in the control loop and how they could

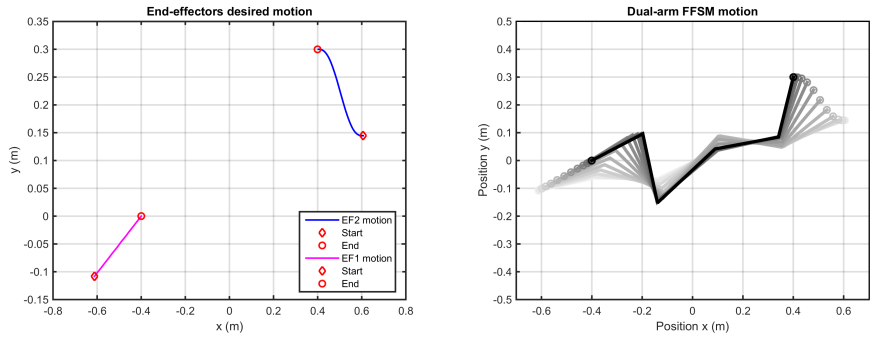

(a) (b)

Figure 2: Reference trajectories for end-effectors and desired motion of the FFSM.

affect the overall performance of the system.

For the sake of comparison, Fig. 3 presents the results obtained for DEM2 with both controllers. Sum of applied torques and $\mathcal{L}_2$ norm of the state vector were used in order to compare both controllers. For the RLQR these indexes were equal to 1.4687 Nm and 0.5536, respectively; for the H_∞ they resulted in 1.5257 Nm and 0.5666, in that order.

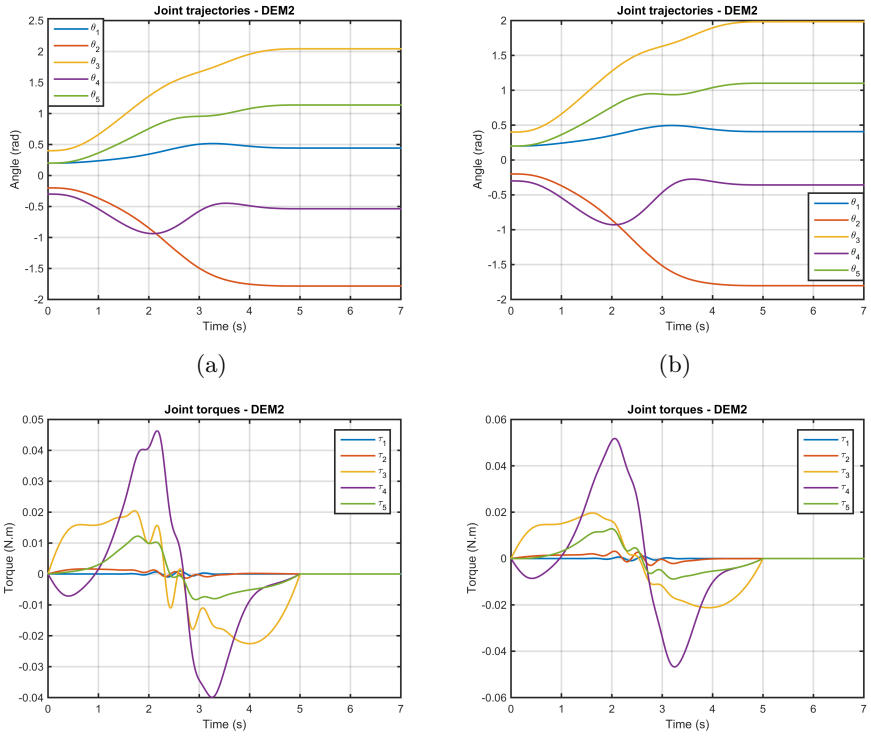

(a) (b)

(c) (d)

Figure 3: Joint trajectories and torques for DEM2 with RLQR and H_∞ controller.

7 Conclusions

In this work, RQLR and robust H_∞ controllers were applied to solve the trajectory tracking problem for a planar dual-arm FFSM. The DEM method was used to model the FFSM through fixed-base underactuated manipulators. The Generalized Jacobian matrices made it possible to map the reference trajectories from workspace into joint space in order to avoid the downsides of inverse kinematics. Even in the presence of parametric uncertainties and disturbances, RLQR and H_∞ controllers were able to successfully accomplish trajectory tracking with small tracking errors. However, the RLQR presented smaller performance indexes for the given reference trajectories, which means that the operation with the RLQR had better disturbance rejection and positioning precision while consuming less energy due to lower torques. Besides, the recursivity of the RLQR makes it a promising controller for real-time applications in space robots and underactuated terrestrial prototypes, since an optimal feedback gain is calculated online for each state. At last, authors would like to thank Capes, CNPq and FAPEAM for financial support.

References

[1] R. A. Bezerra, Modelling and control of a free-floating space manipulator with two arms (in Portuguese), Master's thesis in Electrical Engineering, USP, (2015).

[2] S. Jia, Y. Jia, S. Xu, Q. Hu, Maneuver and Active Vibration Suppression of Free-Flying Space Robot, IEEE Transactions on Aerospace and Electronic Systems, vol. 54, 1115–1134, (2018), DOI: 10.1109/TAES.2017.2775780.

[3] B. Liang, Y. Xu and M. Bergerman, Dynamically equivalent manipulator for space manipulator system. 1, Proceedings of International Conference on Robotics and Automation, vol. 4, 2765–2770, (1997), DOI: 10.1109/ROBOT.1997.606705.

[4] T. F. P. A. T. Pazelli, Assembly and Nonlinear H_∞ Control of Free-Floating Space Manipulators (in Portuguese), PhD thesis in Electrical Engineering, USP, (2011).

[5] A. Seddaoui, C. M.Saaj and S. Eckersley, Adaptive H_∞ Controller for Precise Manoeuvring of a Space Robot, 2019 International Conference on Robotics and Automation (ICRA), 4746–4752, (2019), DOI: 10.1109/ICRA.2019.8794374.

[6] A. A. G. Siqueira, M. H. Terra and M. Bergerman, Robust Control of Robots: fault tolerant approaches, Springer-Verlag, Cap. 2, (2011).

[7] M. H. Terra, J. P. Cerri and J. Y. Ishihara, Optimal Robust Linear Quadratic Regulator for Systems Subject to Uncertainties, IEEE Transactions on Automatic Control, vol. 59, 2586–2591, (2014), DOI: 10.1109/TAC.2014.2309282.

[8] K. Yoshida, A general formulation for under-actuated manipulators, Proceedings of the 1997 IEEE/RSJ International Conference on Intelligent Robot and Systems. Innovative Robotics for Real-World Applications (IROS), vol. 3, 1651–1657, (1997), DOI: 10.1109/IROS.1997.656579.